Science Advances

AAAS

advances.sciencemag.org/cgi/content/full/2/2/e1501250/DC1

Supplementary Materials for

Resolving thermoelectric "paradox" in superconductors

Connor D. Shelly, Ekaterina A. Matrozova, Victor T. Petrashov

Published 26 February 2016, *Sci. Adv.* **2**, e1501250 (2016)
DOI: 10.1126/sciadv.1501250

The PDF file includes:

Calculating thermoelectric flux

As was mentioned in the main text the application of a temperature gradient to a superconductor creates a phase difference $\Delta\theta = \left(2m\eta_q / e\hbar n_s\right)\Delta T$ across the superconductor (4) that is analogous to the difference in electrochemical potential across the ends of a normal metal placed in a temperature gradient. In previous theories (3, 4, 16) the thermoflux was directly connected to the phase difference, $\Delta\theta$. Calculation of the circulating current, which generates the thermoelectric magnetic field, B_{Th}, and the corresponding magnetic flux, Φ_{Th} , was not attempted. In this paper we report on such calculations.
The **Eq. 1** connects the thermoelectric flux and the circulating current

$$\Phi_{Th} = L_2 I_{cs} \tag{1}$$

We consider a superconducting thermocouple consisting of a superconductor, *S*, and a superconductor, *S'*, with much larger gap and hence negligible quasiparticle current. This situation corresponds with our experiments; however it is simple to generalise it to an arbitrary superconductor *S'*.

When the thermocouple is open-circuited the total current in each superconductor must be zero. This is automatically achieved, since the thermoelectric quasiparticle current $I_q=j_q s$ is completely compensated by the counter-flowing supercurrent $I_s=j_s s$, so the total current $I_q + I_s = 0$; *s* is the cross-sectional area of the superconductor. The supercurrent, I_s, is carried by Cooper pairs that can penetrate from *S* into *S'* without any impediments while the current I_q cannot, since there are no allowed states for quasiparticles on the *S'* side. The quasiparticle current is transformed into a supercurrent on the *S'* side (Fig. S1 A) via an unusual process called "Andreev reflection" (34). During Andreev reflection a Cooper pair is created on the *S'* side when an electron incident at the interface is paired with another electron creating a hole on the *S* side (Fig. S1). In real space the hole retraces the electron path (Fig. S1 A). A Cooper pair is annihilated on the *S'* side when a hole incident at the interface is annihilated by one of the electrons of a Cooper pair while the second electron is excited to a quasiparticle state (Fig. S1 B). In real space the electron retraces the hole path (Fig. S1 A). In equilibrium the numbers of Cooper pairs created and annihilated are equal and the total current through the interface is zero. When quasiparticle thermoelectric current is generated, the Andreev reflection converts it to an equal supercurrent, $I_{s'}$, on the *S'* side making the total current $I_{s'} + I_s = 0$ (Fig. S1 A).

When the two ends of the superconducting thermocouple are connected together, a circulating current, I_{cs}, is induced. It flows in the inner Λ-layer of the loop (Fig. 1 A) and obeys the current conservation requirement

$$I_q(x) + I_s(x) = I_{cs} = const \tag{SE1}$$

where *x* is the coordinate along the bimetallic loop. The circulating current reduces the energy of the bimetallic loop therefore its existence is energetically favourable (13).

According to (13) the total energy, *W*, of the loop consists of the energy of the magnetic field $W_m = L_2 I_{cs}^2/2$ created by the circulating current and the kinetic energy $W_k = L_k(x) I_s^2(x)/2$ of superconducting electrons in *S*, with

$$W = \int_0^{l_0} \left(dW_k(x)/dx\right)dx + W_m \tag{SE2}$$

L_k is the kinetic inductance, x=0 at the hot end, l_0 is the length of the superconductor, *S*. Taking into account the requirement that *each* current be continuous across the cold interface at $x=l_0$: $I_q(l_0) = 0$, $I_s(l_0) = I_{cs}$ we arrive at

$$W = L_k(0)\left[I_{cs} - I_q(0)\right]^2/2 - L_k(l_0) I_{cs}^2/2 + L_2 I_{cs}^2/2 \tag{SE3}$$

where $I_q(0)$ and $L_k(0)$ correspond to the hot contact. Minimizing *W* with respect to I_{cs} by solving equation $\partial W/\partial I_{cs} = 0$, we obtain

$$I_{cs} = I_q(0) L_k(0)/\left(L_2 + \delta L_k\right) \tag{SE4}$$

where $\delta L_k = L_k(0) - L_k(l_0)$, $I_q = -\eta_q s\left(dT_q/dx\right)$, η_q is the thermoelectric coefficient,

T_q is the temperature of quasiparticles.
The quasiparticle temperature gradient, dT_q/dx, can be calculated using the heat equation:

$$-\frac{d}{dx}\left(\kappa_q s \frac{dT_q}{dx}\right)dx = \Sigma s\left(T_q^n - T_p^n\right)dx \tag{SE5}$$

The left hand side of the equation is the rate at which the quasiparticles accumulate energy in the volume *sdx* of the wire from the heat flow $\dot{Q}_q = \kappa_q s\left(dT_q/dx\right)$, and the right hand side is the rate of quasiparticle energy transfer to the phonons in the wire, $\dot{Q}_{qp} = \Sigma s\left(T_q^n - T_p^n\right)dx$; κ_q is the quasiparticle thermal conductivity, T_p is the phonon temperature; Σ is a material electron-phonon interaction parameter (18), n=5 or 6 depending on the relationship between the electron mean free path, l, and the phonon wavelength, λ_p (19).

Integrating (SE5) over the length l_0 we obtain

$$\kappa_q s \left.\frac{dT_q}{dx}\right|_{x=0} - \kappa_q s \left.\frac{dT_q}{dx}\right|_{x=l_0} = s\left\langle \Sigma\left(T_q^n - T_p^n\right)\right\rangle l_0 \tag{SE6}$$

Since the quasiparticle concentration in the superconductor *S'* is negligibly small and the heat flow through the cold contact at $x=l_0$ is insignificant, the value of the temperature gradient at the hot contact is

$$dT_q/dx = \left(1/\kappa_q(0)\right)\left\langle \Sigma\left(T_q^n - T_p^n\right)\right\rangle l_0 \qquad \text{(SE7)}$$

where $\langle ... \rangle$ means average over the length l_0:

$$\left\langle \Sigma\left(T_q^n - T_p^n\right)\right\rangle = \frac{1}{l_0}\int_0^{l_0} \Sigma\left(T_q^n - T_p^n\right) dx \qquad \text{(SE8)}$$

In superconductors, due to existence of the energy gap, the coefficients $\eta_q(0), \kappa_q(0)$ and Σ drop exponentially with temperature together with the quasiparticle concentration. They are connected to their normal values by a function, $G(T_q)$, describing the quasiparticle concentration drop with $\eta_q(0) = \eta_N(0)G(T_q(0))$ (3), $\kappa_q(0) = \kappa_N(0)G(T_q(0))$ (20), $G(z) = \left(3/2\pi^2\right)\int_z^\infty y^2 dy/ch^2(y/2)$ where $z = \Delta(T_q)/k_B T_q \approx 3\left(T_c/T_q\right)\sqrt{1-T_q/T_c}$, T_c is the critical temperature of the smaller gap superconductor, *S*, (34). The temperature dependence of electron-phonon interaction was investigated in (21) and it was found that $\Sigma = \Sigma_N G'(T_q)$ where $G'(T_q)$, similar to $G(T_q)$, is equal to unity at temperatures close to critical and exponentially decreases at lower temperatures. Here we interpolate $G'(T_q)$ with $G(T_q)$, so $\left\langle \Sigma\left(T_q^n - T_p^n\right)\right\rangle = \Sigma_N \left\langle G(T_q)\left(T_q^n - T_p^n\right)\right\rangle$. Using the equality $\eta_N(0) = \alpha_N \sigma_N T_q(0)$, where α_N and σ_N are the thermopower and conductivity in the normal state and assuming that the normal state quasiparticle thermal conductivity obeys the Wiedemann-Franz law $\kappa_N(0) = \sigma_N \mathcal{L} T_q(0)$, $\mathcal{L} = 2.4\cdot 10^{-8}$ V^2K^{-2} is the Lorenz number, we arrive at the **Equation 2** for the thermoelectric flux:

$$\Phi_{Th} = -\alpha_N \Sigma_N \left\langle G(T_q)\left(T_q^n - T_p^n\right)\right\rangle L_{eff} \mathcal{V} / \mathcal{L} \qquad (2)$$

Where $L_{eff} = L_2 L_k(0)/\left(L_2 + \delta L_k\right)$ is the effective inductance, $\mathcal{V}$ is the volume of the small gap superconductor. The kinetic inductance at the cold end, $L_k(l_0)$ is estimated to be much smaller than $L_k(0)$ so we discount it, hence $L_{eff} = L_2 L_k(0)/\left(L_2 + L_k(0)\right)$.

Note that the thermoflux depends on the quasiparticle concentration in the bulk of aluminium; it is not directly dependent of the conductivity, however depends on sample properties via α_n and L_{eff}. The phonon term, T_p^n, in the difference, $T_q^n - T_p^n$, entering the formula can be neglected (see the main text). When the temperature of the hot end approaches T_c the effective inductance approaches the value of geometrical inductance of the bimetallic loop:

$L_{eff}(T_c) = L_2 L_k(0) \big/ \left(L_2 + L_k(0) - L_k(l_0)\right) \to L_2$ since $L_k(0) = \Phi_0 / 2\pi I_c(0) \to \infty$ at $I_c(0) \to 0$. The absolute value of thermoelectric flux (2) at temperatures close to critical is therefore

$$\Phi_{Th}(T_c) \approx \alpha_N \Sigma_N \left\langle T_c^n \right\rangle L_2 \mathcal{V} / \mathcal{L} \qquad \text{(SE9)}$$

At temperatures below critical, the value of thermoflux can be written as

$$\Phi_{Th}(T_q) = \Phi_{Th}(T_c) \left\langle G(T_q / T_c) \cdot \left(T_q / T_c\right)^n \right\rangle \left(L_{eff} / L_2\right) \qquad \text{(SE10)}$$

It goes to zero due to a decrease in the three scaling factors: the $G(T_q/T_c)$-function that describes the drop in the quasiparticle concentration, the electron-phonon scattering rate ($(T_q/T_c)^n$ factor) and the kinetic inductance ((L_{eff}/L_2) factor) that decreases as a result of increase of the critical current

Fig. S2 shows the temperature dependence for all three scaling factors. To fit experimental data in Fig. 3 B of the main text we have taken n=6 (see main text) with $\alpha_N = 2 \cdot 10^{-8}$ V/K^2, $\Sigma_N \approx 5 \cdot 10^{10}$ Wm^{-3}K^{-6} and the dependence of critical current at the hot contact in the form $I_c = I_0 \left(1 - T_q(0) / T_c\right)$ (26) with a fitting parameter I_0=30 μA. The sensitivity of thermoflux to the choice of parameters n and I_0 can be seen from Fig. S3 showing theoretical temperature dependence of the thermoflux normalized to its value at critical temperature, $\Phi_{Th}(T_q) / \Phi_{Th}(T_c)$, at different n and I_0. The dependence changes essentially with the change of critical current, I_0, while the changes are relatively small when n=6 is substituted with n=5 (see Fig. S3 and the main text).

Thermometry

To measure the temperature at the hot end, $T_q(0)$, we used the superconducting/normal/ superconducting (SNS) junction (32). The thermometer was placed away from the hot contact at the point g to avoid coupling of the thermometer wires to bimetallic and interferometer loops. To make the temperatures at g and e (see Fig. 2 c of the main text) close to each other the thermal coupling of the heater to the thermometer and the bimetallic loop were made similar. The point g and the point e were connected to the heater at point f by the normal silver wires of the same length and width with similar thermal boundary conditions at the superconductors. The temperature distribution in both wires obeyed heat equations similar to **Equation S6**:

$$\sigma \mathcal{L} T_q \left.\frac{dT_q}{dx}\right|_f = \Sigma \left\langle T_q^n - T_p^n \right\rangle l_c + \kappa \left.\frac{dT_q}{dx}\right|_g \qquad \text{(SE11)}$$

where κ, Σ, T_q, T_p and σ are the thermal conductivity, electron-phonon coupling constant , electron and phonon temperatures, and the conductivity of silver; $\mathcal{L}$ is the Lorenz number, l_c

is the length of the connecting wire. The term $\sigma \mathcal{L} T_q \, dT_q/dx\big|_f$ on the left is the thermal flux generated by the heater current at *f*. Within the heater wire the Joule heat contribution, j^2/σ, should be added to the heat equation, *j* is the heater current density. When both connecting wires and their boundary conditions are identical then the thermometer temperature close to *g* and the temperature at the hot contact, *e*, are equal, $T_q\big|_g = T_q\big|_e$, at any heater current.

The actual boundary conditions do not completely coincide. In our case the boundary conditions at the superconductors may depend on the quality and geometry of the N/S contacts. As a result the same values of temperatures $T_q\big|_g$ and $T_q\big|_e$ may be reached at different heater currents, I_h' and I_h. As in general when the sensor and the sample cannot be placed in the same point tooling factors should be taken into account.

The SNS thermometer operated in a highly temperature-sensitive resistive state with negligible proximity induced critical current. To ensure this we have investigated the dependence of the critical current on the length of the normal segment shown in Fig. S4.

Examples of the plots of the thermometer differential resistance *vs* bias current at different temperatures and heater currents are shown in Figs. S5 and S6.

The values of the differential resistance at zero bias were used to plot the temperature increment $\Delta T = T_q - T_0$ *vs* heater current, I_h; T_0 is the bath temperature. The dependence ΔT vs heater current normalized to its value, I_h^c, at the onset of superconductivity in aluminium, is shown in Fig. S7 for different thermometers. The dependence follows a universal function that can be used as a calibration curve. To find the value of ΔT in a particular device, the normalized value should be multiplied by the directly measured value of I_h^c. The connection of the hot contact of the bimetallic loop to the heater was similar to that of the thermometer so the ΔT *vs* normalised heater current dependence of Fig. S7 can be used to find ΔT at the hot contact of bimetallic loop at a given heater current if the value I_h^c is known.

We found the value I_h^c for the loop during thermocycling that is described in the main text. Fig. S8 shows the dependence of the interferometer resistance as a function of the heater current at a fixed magnetic field. The steep change in the resistance corresponds to the change in the phase of oscillations when the trapped flux escapes the loop and the resistance jumps from one oscillating curve, shown in Fig. 2 A, to another. At this value of the heater current the penetration depth, Λ, reaches the width of the aluminium wire, *w*. Using the directly measured Λ vs T curves, which were found to follow the equation $\Lambda(nm) = 65/(1-(T_c/T)^4) \pm 5$, in agreement with Pearl's theory (see e.g. (33) and references therein) we found that the penetration depth reaches $\Lambda = w = 0.7$ μm at the temperature $T \approx 0.98 T_c$ that is very close to the critical value giving $I_h^c \approx 42$ μA for the loop.

Figures.

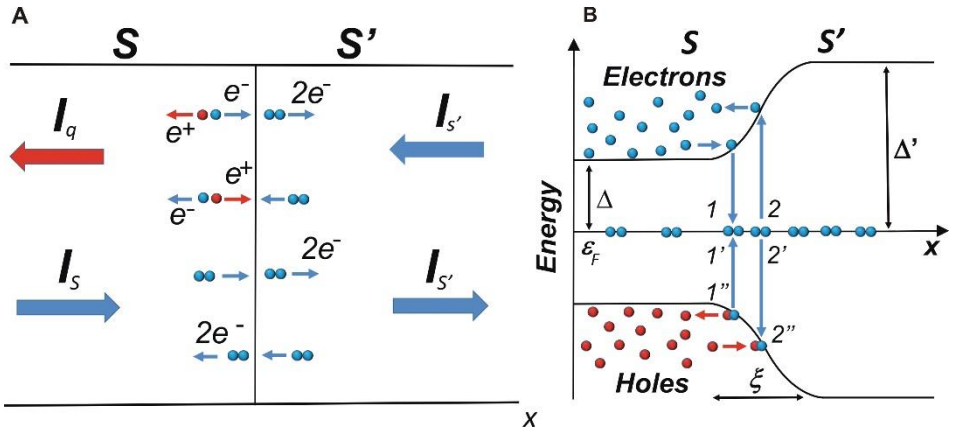

Figure S1. Conversion of currents at the interface between two superconductors, *S* and *S'*, with different energy gaps, Δ and Δ'.

(A) Andreev reflection processes at the *SS'* interface in real space; an incident electron evolves into a hole, which retraces the electron trajectory on the *S* side, and a Cooper pair is created on the *S'* side; an incident hole evolves into an electron, which retraces the hole trajectory on the *S* side, and a Cooper pair is annihilated on the *S'* side; the Cooper pairs commute between the superconductors unrestrained; a quasiparticle current, I_q on the *S* side (red arrow) is converted to an equal supercurrent $I_{s'}$ on the *S'* side, counter-flowing supercurrent I_s on the S side (blue arrow) penetrates to *S'* unrestricted. (**B)** Sketch of the energy-band diagram at the interface, ε_F is the Fermi level; process 1–1' corresponds to creation of a Cooper pair with simultaneous creation of a hole at 1''; 2–2' is annihilation of a Cooper pair with simultaneous annihilation of a hole at 2''; ξ is the crossover region.

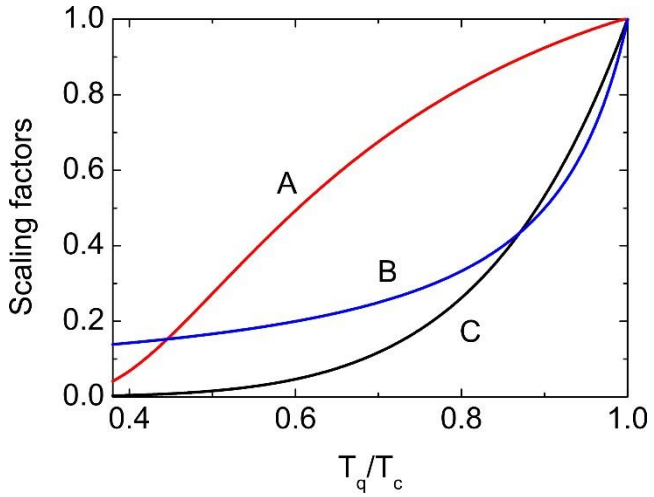

Fig. S2. Calculated dependence of the thermoelectric flux scaling factors on the quasiparticle temperature normalized to critical temperature, T_c. A - G-function describing quasiparticle concentration; B - effective iductance, L_{eff}, normalized to the geometric inductance of bimetallic loop, L_2; C – the value of $(T_q/T_c)^6$.

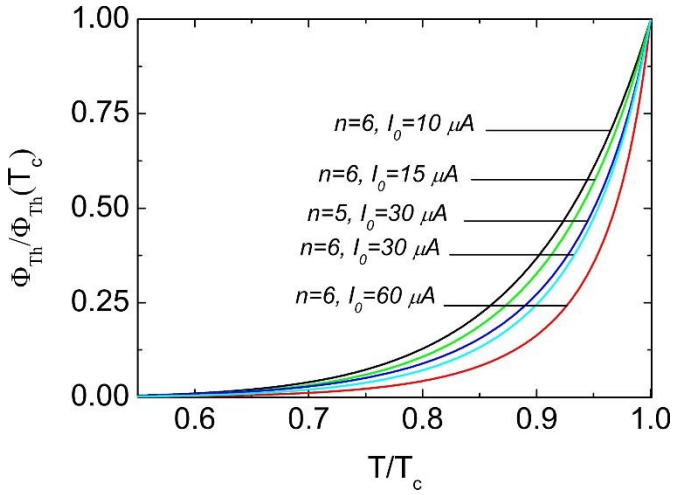

Fig. S3. Calculated temperature dependence of thermoelectric flux, Φ_{th}, normalized to its value, $\Phi_{th}(T_c)$, at critical temperature with different values of critical current, I_0, and electron-phonon parameter, n.

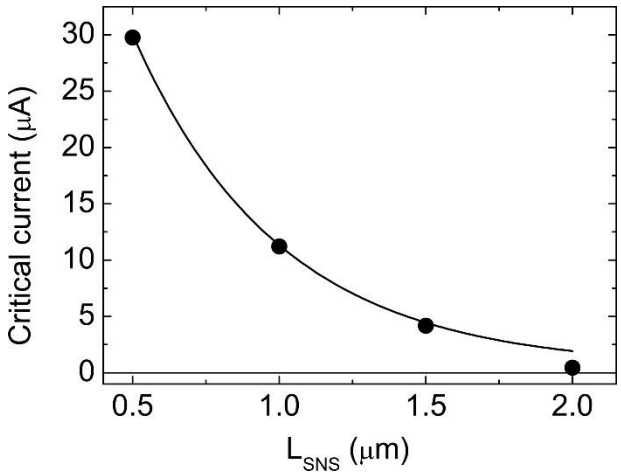

Fig. S4. Dependence of critical current in SNS thermometer on the length of normal element at base temperature T=245 mK. Solid line is for eye guide.

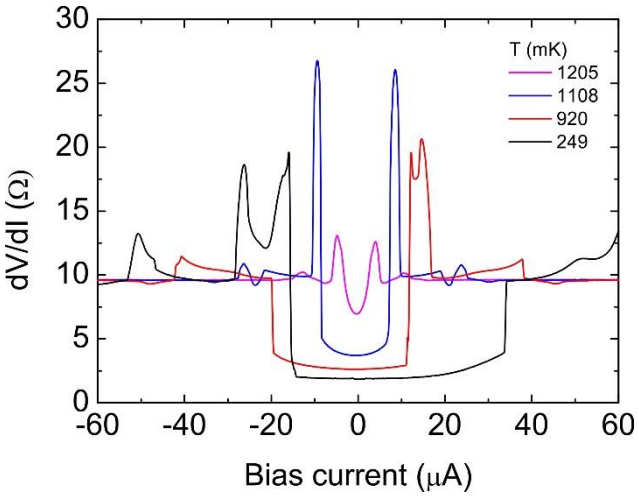

Fig. S5. Differential resistance *vs* bias current curves for an SNS thermometer at different bath temperatures.

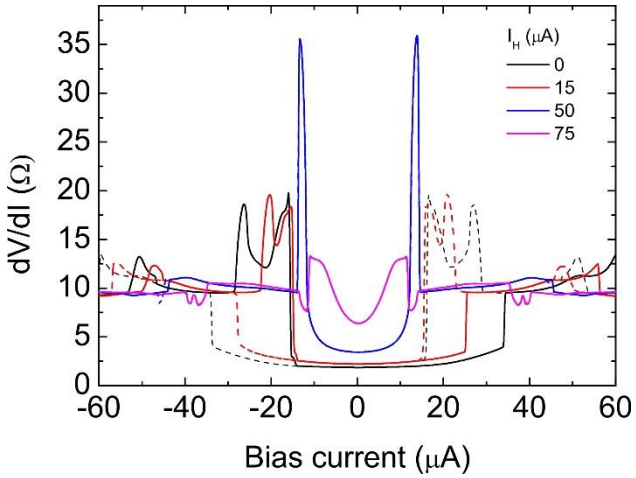

Fig. S6. Differential resistance *vs* bias current curves for an SNS thermometer at different heater currents.

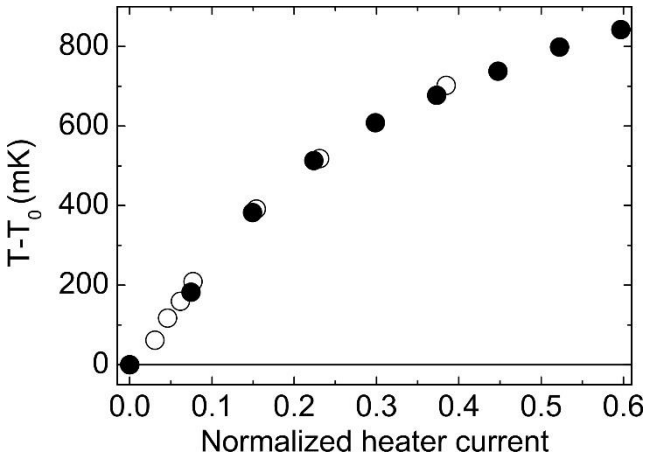

Fig. S7. Temperature calibration curve.

Temperature increment, $\Delta T = T - T_0$, measured by different thermometers *vs* normalized heater current, I_h / I_h^c; I_h^c is the value of the heater current at the onset of superconductivity in aluminium; T_0 is the temperature at zero heater current; ○ - ΔT for a thermometer with $I_h^c = 48$ μA, ● ΔT for a thermometer with $I_h^c = 63$ μA.

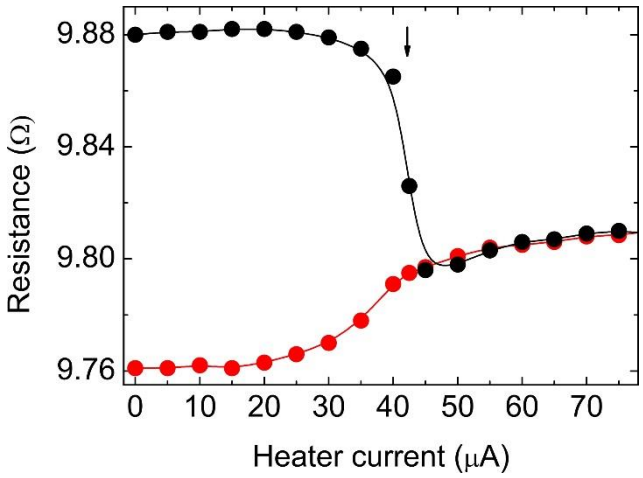

Fig. S8. Determination of the heater current corresponding to the onset of superconductivity in the bi-metallic loop. Interferometer resistance at a fixed magnetic field *vs* heater current. The steep change in the resistance (shown with arrow) takes place at the onset of superconductivity in the aluminium wire of bimetallic loop at the heater current $I_h^c \approx 42$ μA.